Mathematical modeling of the fluid flow and geo-mechanics in the fractured porous media using generalized multiscale finite element method

Cite as: AIP Conference Proceedings **2025**, 100009 (2018); https://doi.org/10.1063/1.5064938
Published Online: 25 October 2018

A. Tyrylgin, M. Vasilyeva, Q. Zhang, D. Spiridonov, and V. Alekseev

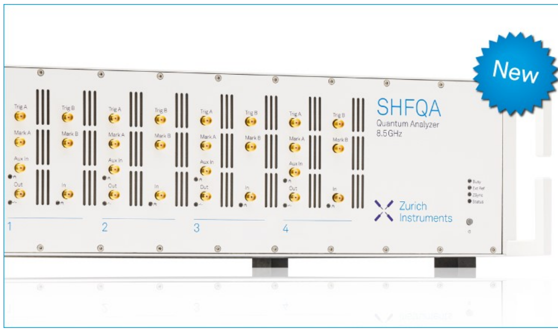

Mathematical Modeling of the Fluid Flow and Geo-mechanics in the Fractured Porous Media using Generalized Multiscale Finite Element Method

A. Tyrylgin[1,a)], M. Vasilyeva[1,2], Q. Zhang[3], D. Spiridonov[1] and V. Alekseev[1]

[1]*MMR Laboratory, North-Eastern Federal University, Yakutsk, Russia*
[2]*ISC, Texas A&M University, College Station, TX, USA and MMR Laboratory, North-Eastern Federal University, Yakutsk, Russia*
[3]*China University of Petroleum (East China), Qingdao, China*

[a)]Corresponding author: koc9tk@mail.ru

Abstract. In the reservoir simulation, mathematical modeling of the fluid flow and geo - mechanics in the fractured porous media plays an important role. Fracture networks have complex geometries, exist in the multiple scales and typically have very small thickness compared to typical reservoir sizes. Due to high permeability, fractures have a significant impact on the flow processes. In this work, we consider a discrete fracture model for coupled flow and mechanics problems. We construct coarse grid approximation using Generalized Multiscale Finite Element method (GMsFEM). In this method, we solve local spectral problems for construction to the multiscale basis functions for pressure and displacements. We present numerical results for two - dimensional model problem.

MATHEMATICAL MODEL

We consider a mathematical model of coupled flow and mechanics in fractured poroelastic medium. The model contains a mass balance equation for the flow and a linear momentum balance equation for the mechanics [1, 3, 9].

The balance of a linear momentum in the solid is given as

$$-\operatorname{div}\sigma_T(u,p) = 0, \quad \sigma_T(u,p) = \sigma(u) - \alpha p \mathcal{I}, \quad x \in \Omega, \tag{1}$$

where u is the displacement, α is Biot's coefficient, p is the fluid pressure, σ_T is the total stress tensor, σ is the linear stress.

Relation between the stress σ and strain ε tensors is given as

$$\sigma(u) = \lambda \varepsilon_v \mathcal{I} + 2\mu\varepsilon(u), \quad \varepsilon(u) = 0.5(\nabla u + (\nabla u)^T),$$

where ε_v is the volumetric strain, and λ and μ are the Lame's coefficients.

The fluid mass conservation is given as follows:

$$\frac{\partial m}{\partial t} + \operatorname{div}(\rho q) = \rho f, \quad q = -\frac{k}{\nu_f}\operatorname{grad} p, \quad x \in \Omega, \tag{2}$$

where m is the fluid mass, q is Darcy velocity, ν_f is the viscosity, ρ is the fluid density, and f is the source term. Here, for simplicity, we neglect the gravitational forces [6, 7].

Due to the motion of the solid skeleton, we have the following relationship

$$\delta m = \rho\delta\phi + \phi\delta\rho + \rho\delta\varepsilon_v = \rho\left(\frac{1}{M}\delta p + \alpha\delta\varepsilon_v\right),$$

Application of Mathematics in Technical and Natural Sciences
AIP Conf. Proc. 2025, 100009-1–100009-7; https://doi.org/10.1063/1.5064938
Published by AIP Publishing. 978-0-7354-1745-8/$30.00

where

$$\frac{1}{M} = \phi c_f + \frac{\alpha - \phi}{K}, \quad c_f = \frac{1}{\rho}\frac{d\rho}{dp},$$

and c_f is the fluid compressibility, M is Biot's modulus, ϕ is the porosity and K is the solid grain stiffness.

For the highly permeable fracture, we should add equation for flow on the fracture. We use the reduced dimension model for the fluid flow on $\gamma \in \mathcal{R}^{(d-1)}$

$$\frac{\partial(m_f b)}{\partial t} + \operatorname{div}(\rho q_f) = \rho[q \cdot n], \quad q_f = -b\frac{k_f}{\nu_f}\operatorname{grad} p_f, \quad x \in \gamma, \tag{3}$$

where b is the fracture aperture ($b > 0$), m_f is the fluid mass in fracture, q_f and p_f are the mass flux and fluid pressure in the fracture. Here, as source term, we have jump in the matrix mass flux in the normal direction $[q \cdot n]$ and suppose linear relationship between flux and pressure difference $[q \cdot n] = \sigma_{fm}(p - p_f)$.

For pororelastic media, we have

$$\frac{\partial(m_f b)}{\partial t} = \frac{\partial(\rho\phi_f b)}{\partial t} = \rho\left(\phi_f\frac{\partial b}{\partial t} + b\frac{1}{M_f}\frac{\partial p_f}{\partial t}\right),$$

where M_f is the Biot modulus for fracture.

We suppose that $\rho = \text{const}$ and $b = \text{const}$. Therefore, we have the following coupled system of equations for displacements, pressure in porous matrix and fractures

$$\begin{aligned} -\operatorname{div}\sigma(u) + \alpha\operatorname{grad} p = 0, \quad x \in \Omega, \\ c_m\frac{\partial p}{\partial t} + \alpha\frac{\partial \varepsilon_v}{\partial t} - \operatorname{div}(a_m\operatorname{grad} p) + \sigma_{mf}(p - p_f) = f, \quad x \in \Omega, \\ c_f\frac{\partial p_f}{\partial t} - \operatorname{div}(a_f\operatorname{grad} p_f) - \sigma_{fm}(p - p_f) = f_f, \quad x \in \gamma, \end{aligned} \tag{4}$$

where

$$c_m = \frac{1}{M}, \quad c_f = \frac{b}{M_f}, \quad a_m = \frac{k}{\nu_f}, \quad a_f = b\frac{k_f}{\nu_f}.$$

DISCRETE SYSTEM ON THE FINE GRID

Let $\mathcal{T}^h$ denote a finite element partition of the domain Ω and Γ_h be the set of all the interior faces between the elements $\mathcal{T}^h$ [10, 11]. We suppose that $\cup_j\gamma_j \subset \Gamma_h$ is the subset of faces that represent fractures, where $j = \overline{1, N_{\text{frac}}}$ and N_{frac} is the number of discrete fractures.

The weak formulation of the elasticity equation for the finite element method is given by

$$\int_\Omega (\sigma(u, p), \varepsilon(v))dx + \int_\Omega \alpha\operatorname{grad} p \cdot v\, dx = 0. \tag{5}$$

For the pressure equations, we suppose the continuity of the matrix and fracture pressures on the fracture surface and using superposition principles, we obtain the following finite element approximation using discrete fracture model (DFM) [2, 8]

$$\begin{aligned} &\int_\Omega c_m\frac{\partial p}{\partial t} z dx + \int_\Omega \alpha\frac{\partial \varepsilon_v}{\partial t} z dx + \int_\Omega a_m\operatorname{grad} p \cdot \operatorname{grad} z\, dx \\ &+ \sum_j\left(\int_{\gamma_j} c_f\frac{\partial p}{\partial t} z_f ds + \int_{\gamma_j} a_f\operatorname{grad} p \cdot \operatorname{grad} z_f\, ds\right) = \int_\Omega f z dx + \sum_j\int_{\gamma_j} f_f z_f dx. \end{aligned} \tag{6}$$

The standard implicit finite difference scheme is used for the time approximation of the pressure equation (6) and we solve following coupled system in the matrix form on the fine grid

$$\frac{1}{\tau}\begin{pmatrix} M & D \\ 0 & 0 \end{pmatrix}\begin{pmatrix} p - \check{p} \\ u - \check{u} \end{pmatrix} + \begin{pmatrix} A & 0 \\ B & K \end{pmatrix}\begin{pmatrix} p \\ u \end{pmatrix} = \begin{pmatrix} F \\ 0 \end{pmatrix}, \qquad (7)$$

where $M = M_m + M_f$, $A = A_m + A_f$

$$M = [m_{ij}], \quad m_{ij} = \int_\Omega c_m \phi_i \, \phi_j \, dx + \sum_l \int_{\gamma_l} c_f \psi_i \, \psi_j \, dx,$$

$$A = [a_{ij}], \quad a_{ij} = \int_\Omega a_m \operatorname{grad} \phi_i \cdot \operatorname{grad} \phi_j \, dx + \sum_l \int_{\gamma_l} a_f \operatorname{grad} \psi_i \cdot \operatorname{grad} \psi_j \, dx,$$

$$K = [k_{ij}], \quad k_{ij} = \int_\Omega \sigma(\Phi_i) : \epsilon(\Phi_j) \, dx,$$

$$D = [d_{ij}], \quad d_{ij} = \int_\Omega \alpha \operatorname{grad} \phi_i \, \Phi_j \, dx, \quad B = [b_{ij}], \quad b_{ij} = \int_\Omega \alpha \operatorname{div} \Phi_i \, \phi_j \, dx,$$

$$F = [f_j], \quad f_j = \int_\Omega f \, \phi_j \, dx + \sum_l \int_{\gamma_l} f_f \, \psi_j \, dx,$$

and Φ_i, ϕ_i, are the two-dimensional linear basis functions for displacements and pressure, ψ_i is the one-dimensional linear basis functions.

COARSE GRID APPROXIMATION USING GMsFEM

Let $\mathcal{T}_H$ be the coarse grid and $\mathcal{T}_H = \bigcup_i K_i$, where K_i is the coarse cell. We start with discussion of the multiscale space construction. In this work, we construct multiscale basis functions for displacements and pressure separately in each local domain ω_i (see Figure 1 for illustration) [4, 5].

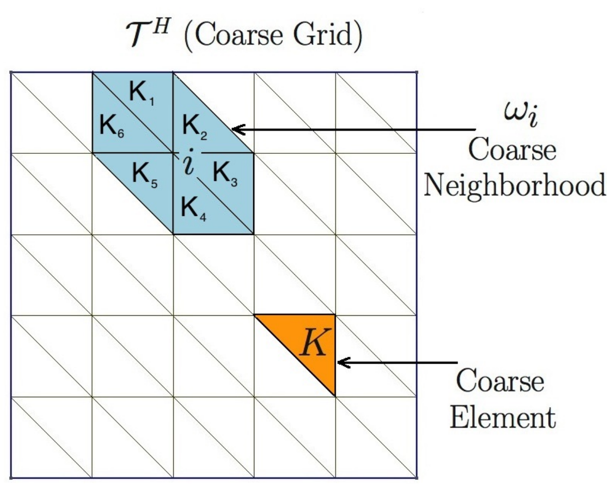

FIGURE 1. Illustration of the coarse grid $\mathcal{T}_H$, local domain ω_i and coarse cell K

Multiscale space. For construction of the multiscale basis functions, we solve a local spectral problems in domain ω_i for displacement and pressure separately. The local spectral problems on ω_i:

- Displacement: $K_\omega \Phi = \lambda_u Q_\omega \Phi$
- Pressure: $A_\omega \phi = \lambda_p S_\omega \phi$

Here K_ω, A_ω are the stiffness matrices for displacements and pressure in local domain ω_i and Q_ω, S_ω are the mass matrices for displacements and pressure

$$Q_\omega = [q_{ij}], \quad q_{ij} = \int\limits_\Omega a_m \phi_i \phi_j \, dx + \sum_l \int\limits_{\gamma_l} a_f \psi_i \psi_j \, dx,$$

$$S_\omega = [s_{ij}], \quad s_{ij} = \int\limits_\Omega (\lambda + 2\mu) \Phi_i \Phi_j \, dx.$$

We choose an eigenvectors ϕ_1, ϕ_2, ..., ϕ_{L_l} and Φ_1, Φ_2,...,Φ_{L_l} corresponding to the first smallest L_l eigenvalues, where $\lambda_1 \le \lambda_2 \le ... \le \lambda_{L_l}$ $(l = u, p)$.

In the fact that the spectral problem must be solved many times. Therefore, it is possible to reduce the dimension of the problem. For solution of the local spectral problem, we use a snapshot space V_{snap} for displacement and Q_{snap} for pressure. We define projection matrices for displacements and for pressure ($R^u_{\text{snap}} = (\phi_1^{\text{snap}}, ..., \phi_{L_i}^{\text{snap}})$ and $R^p_{\text{snap}} = (\Phi_1^{\text{snap}}, ..., \Phi_{L_i}^{\text{snap}})$) and solve following eigenvalue problem on the snapshot space

- Displacement:
$$\overline{K}_\omega \overline{\Phi} = \lambda_u \overline{Q}_\omega \overline{\Phi}, \quad \overline{K}_\omega = R^u_{\text{snap}} K_\omega (R^u_{\text{snap}})^T, \quad \overline{Q}_\omega = R^u_{\text{snap}} Q_\omega (R^u_{\text{snap}})^T,$$
where $\Phi_j^\omega = (R^u_{\text{snap}})^T \overline{\Phi}_j$.
- Pressure:
$$\overline{A}_\omega \overline{\phi} = \lambda_p \overline{S}_\omega \overline{\phi}, \quad \overline{A}_\omega = R^p_{\text{snap}} A_\omega (R^p_{\text{snap}})^T, \quad \overline{S}_\omega = R^p_{\text{snap}} S_\omega (R^p_{\text{snap}})^T,$$
where $\phi_j^\omega = (R^p_{\text{snap}})^T \overline{\phi}_j$.

For obtaining conforming basis functions we use linear partition of unity functions. We construct projection matrices R_u and R_p from a fine grid to a coarse grid and use it for reducing the dimension of the problem

$$R_u = (\chi^1 \Phi_1^1, \chi^1 \Phi_2^1, ..., \chi^1 \Phi_L^1, ..., \chi^{N_c} \Phi_1^{N_c}, \chi^{N_c} \Phi_2^{N_c}, ..., \chi^{N_c} \Phi_L^{N_c})^T,$$

$$R_p = (\chi^1 \phi_1^1, \chi^1 \phi_2^1, ..., \chi^1 \phi_L^1, ... \chi^{N_c} \phi_1^{N_c}, \chi^{N_c} \phi_2^{N_c}, ..., \chi^{N_c} \phi_L^{N_c})^T,$$

where χ^i is linear partition of unity functions, $L = L_p = L_u$ is the number of basis functions and N_c is the number of vertices of a coarse grid.

Then the system of equations can be translated into a coarse grid

$$\frac{1}{\tau} \begin{pmatrix} M_c & D_c \\ 0 & 0 \end{pmatrix} \begin{pmatrix} p_c - \check{p}_c \\ u_c - \check{u}_c \end{pmatrix} + \begin{pmatrix} A_c & 0 \\ B_c & K_c \end{pmatrix} \begin{pmatrix} p_c \\ u_c \end{pmatrix} = \begin{pmatrix} F_c \\ 0 \end{pmatrix}, \tag{8}$$

where $K_c = R_u K R_u^T$, $A_c = R_p A R_p^T$, $M_c = R_p M R_p^T$, $B_c = R_u B R_p^T$, $D_c = R_p D R_u^T$ $F_c = R_p F$. After obtaining of a coarse-scale solution, we can reconstruct fine-scale solution $u_{ms} = R_u^T u_c$ and $p_{ms} = R_p^T p_c$.

NUMERICAL RESULTS

Calculations performed on a computation domain, which is shown in Figure 2. We set $\Omega = [0, 50]^2$. Fine grid consists 12944 vertices, 25486 cells and 38429 facets and coarse grid contains 121 vertices.

The numerical solution is presented for the following boundary conditions

$$u_x = 0, \ \sigma_y = 0, \ x \in \Gamma_3 \cup \Gamma_1 \quad u_y = 0, \ \sigma_x = 0, \ x \in \Gamma_4 \cup \Gamma_2 \quad p = 1, \ x \in \Gamma_1.$$

The calculation is performed by $T_{max} = 0.1$ with step in time $\tau = 0.01$.

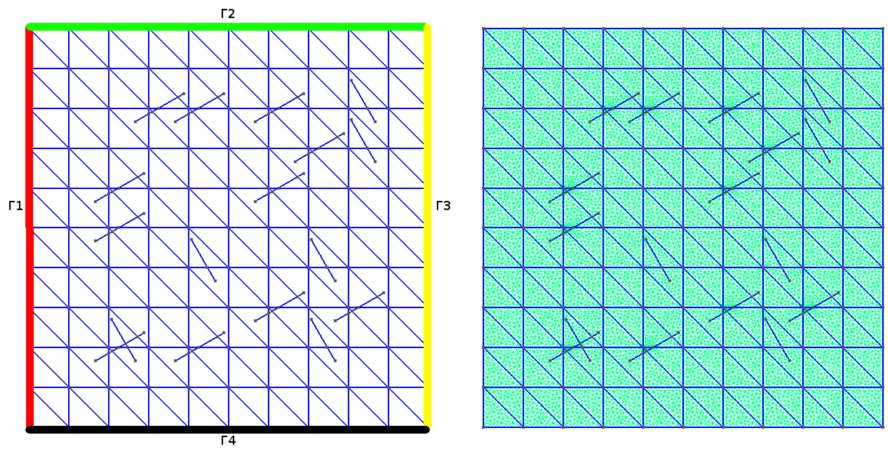

FIGURE 2. Computation meshes. Left: coarse grid. Right: fine grid

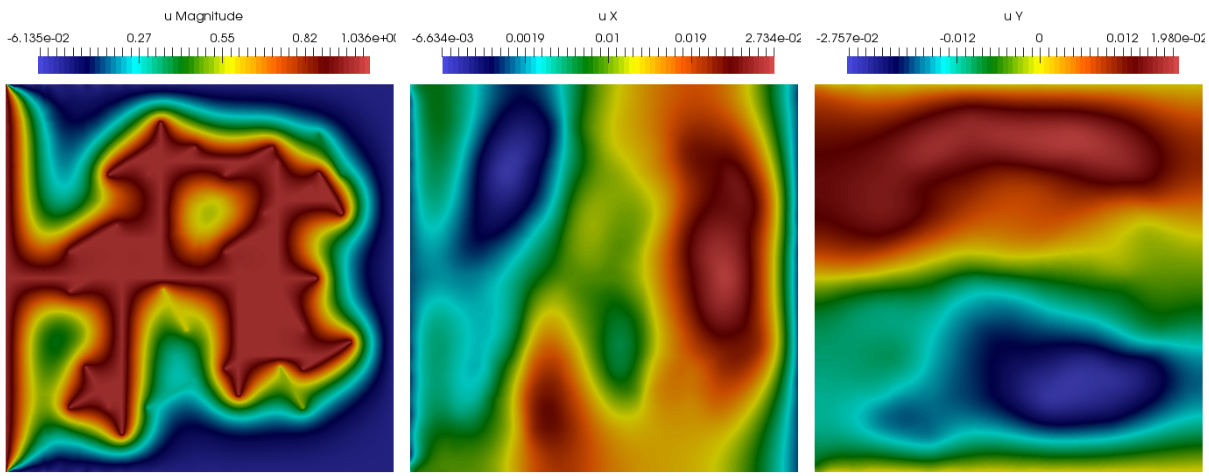

FIGURE 3. Distribution of pressure, displacement along X and Y directions at the last moment of time in homogeneous fractured porous media

TABLE 1. Relative errors for displacement and pressure with different numbers of multiscale basis functions for GMsFEM in homogeneous fractured porous media

L	L_2^u (%)	H_1^u (%)	L_2^p (%)	H_1^p (%)
1	81.7277	77.8344	51.7067	127.035
2	30.8361	49.2153	29.7308	93.3461
4	7.31921	14.7866	6.71832	39.985
8	2.3319	5.65635	0.985431	12.5086
12	1.69256	5.59024	0.339608	7.26006

Homogeneous Fractured Porous Media

In this section, we present numerical results of coupled flow and mechanics in fractured poroelastic medium with homogeneous background media properties. We set $E = 10$ and $k = 0.01$. We set Biot modulus $\beta = 0.1$, Biot coefficient $\alpha = 0.1$.

In Figure 3, we present the distribution of pressure and displacement along the X and Y directions at the last moment of time for the fine grid solution in homogeneous media. In Table 1, we present the weighted L^2 and H^1 errors for multiscale solver.

Heterogeneous Fractured Porous Media

Let us perform a numerical simulation of the considered problem of poroelasticity in heterogeneous media. We set Biot modulus $\beta = 0.01$, Biot coefficient $\alpha = 1$. Elasticity parameter and heterogeneous permeability are presented in Figure 4.

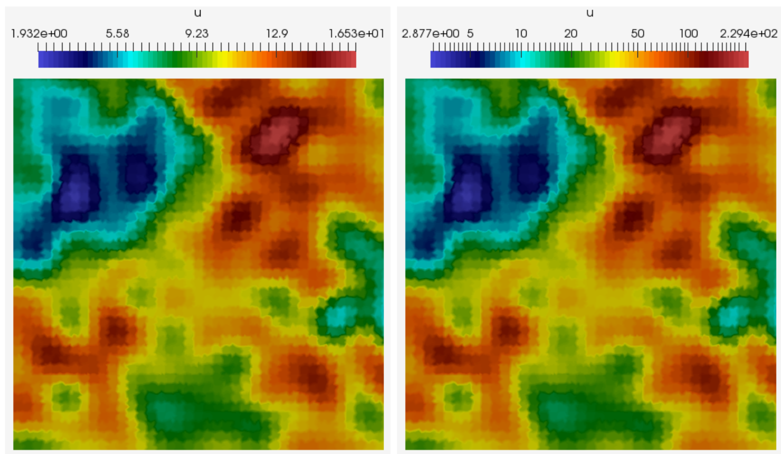

FIGURE 4. Elasticity parameter E(left) and heterogeneous permeability k(right)

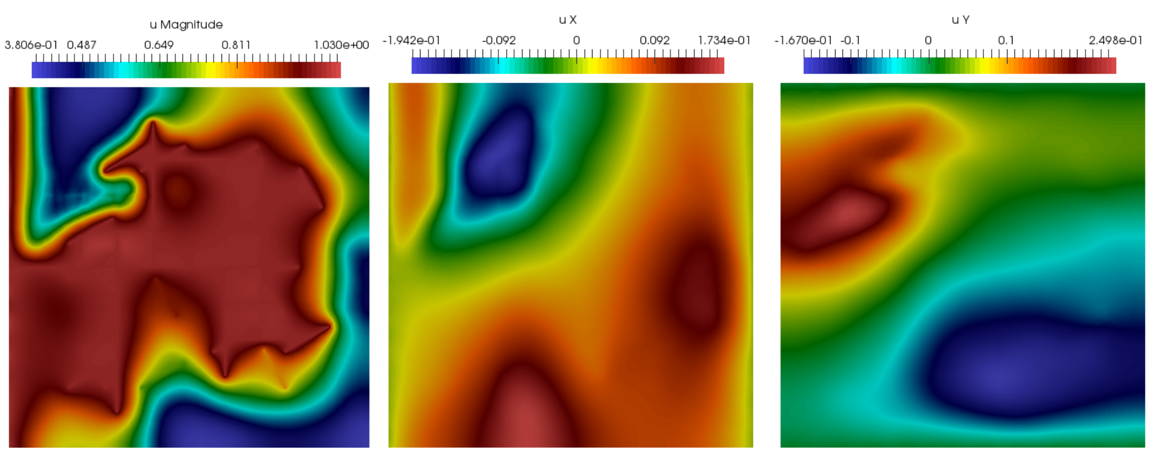

FIGURE 5. Distribution of pressure, displacement along X and Y directions at the last moment of time in heterogeneous fractured porous media

In Figure 5, we present the distribution of pressure and displacement along the X and Y directions at the last moment of time for the fine grid solution in heterogeneous media. In Table 2, we present the weighted L^2 and H^1 errors for multiscale solver.

We obtain accurate solution using a small number of the multiscale basis functions for both cases. In future works, we will consider dual continuum backround media and consider three-dimensional test cases.

TABLE 2. Relative errors for displacement and pressure with different numbers of multiscale basis functions for GMsFEM in heterogeneous fractured porous media

L	L_2^u (%)	H_1^u (%)	L_2^p (%)	H_1^p (%)
1	80.9641	69.2054	14.951	141.648
2	23.159	41.3603	11.5642	102.523
4	11.1475	14.2097	2.71181	34.5921
8	5.63175	10.4813	3.60061	29.3502
12	1.14291	5.16293	0.460655	6.42927

ACKNOWLEDGEMENTS

Work is supported by the mega-grant of the Russian Federation Government (No 14.Y26.31.0013) and grant of the Russian Scientific Found (No 17-71-20055).

REFERENCES

[1] I.Y. Akkutlu, Y. Efendiev, M. Vasilyeva, and Y. Wang (2018) Multiscale model reduction for shale gas transport in poroelastic fractured media, *Journal of Computational Physics* **353**, 356–376.

[2] M.Vasilyeva, E.T. Chung, W.T. Leung, and V. Alekseev (2018) Nonlocal multicontinuum (NLMC) upscaling of mixed dimensional coupled flow problem for embedded and discrete fracture models, arXiv:1805.09407, 2018.

[3] M. Vasilyeva, E.T. Chung, Y. Efendiev, and J. Kim, Constrained energy minimization based upscaling for coupled flow and mechanics, arXiv:1805.09382, 2018.

[4] D.L. Brown and M. Vasilyeva (2016) A generalized multiscale finite element method for poroelasticity problems II: Nonlinear coupling, *Journal of Computational and Applied Mathematics* **294**, 372–388.

[5] D.L. Brown and M.V. Vasilyeva (2016) A generalized multiscale finite element method for poroelasticity problems I: Linear problems, *Journal of Computational and Applied Mathematics* **297**, 132–146.

[6] A.E. Kolesov, P.N. Vabishchevich, and M.V. Vasilyeva (2014) Splitting schemes for poroelasticity and thermoelasticity problems, *Computers & Mathematics with Applications* **67**(12), 2185–2198.

[7] G.I. Barenblatt, Yu.P. Zheltov, and I.N. Kochina (1960) Basic concepts in the theory of seepage of homogeneous liquids in fissured rocks (strata), *Journal of applied Mathematics and Mechanics* **24**(5), 1286–1303.

[8] V. Girault, K. Kumar, and M.F. Wheeler (2016) Convergence of iterative coupling of geomechanics with flow in a fractured poroelastic medium, *Computational Geosciences* **20**(5), 997–1011.

[9] J. Kim, H.A. Tchelepi, and R. Juanes (2011) Stability and convergence of sequential methods for coupled flow and geomechanics: Drained and undrained splits, *Computer Methods in Applied Mechanics and Engineering* **200**(23), 2094–2116.

[10] A. Logg, K.-A. Mardal, and G. Wells, *Automated Solution of Differential Equations by the Finite Element Method: The FEniCS book*, Vol. **84** (Springer Science & Business Media, 2012).

[11] Computing platform FEniCS (http://fenicsproject.org).